Corticolimbic Interactions Associated with Performance on a Short-Term Memory Task Are Modified by Age

Valeria Della-Maggiore,[1] Allison B. Sekuler,[2] Cheryl L. Grady,[1] Patrick J. Bennett,[2] Robert Sekuler,[3] and Anthony R. McIntosh[1]

[1]Rotman Research Institute of Baycrest Centre, Toronto, Ontario M6A 2E1, Canada, [2]Department of Psychology, University of Toronto, Toronto, Ontario, M5S 2G3, Canada, and [3]Volen Center for Complex Systems, Brandeis University, Waltham, Massachusetts

Aging has been associated with a decline in memory abilities dependent on hippocampal processing. We investigated whether the functional interactions between the hippocampus and related cortical areas were modified by age. Young and old subjects' brain activity was measured using positron emission tomography (PET) while they performed a short-term memory task (delayed visual discrimination) in which they determined which of two successively presented sine-wave gratings had the highest spatial frequency. Behavioral performance was equal for the two groups. Partial least squares (PLS) analysis of PET images identified a hippocampal voxel whose activity was similarly correlated with performance across groups. Using this voxel as a seed, a second PLS analysis identified cortical regions functionally connected to the hippocampus. Quantification of the neural interactions with structural equation modeling suggested that a different hippocampal network supported performance in the elderly. Unlike the neural network engaged by the young, which included prefrontal cortex Brodmann's area (BA) 10, fusiform gyrus, and posterior cingulate gyrus, the network recruited by the old included more anterior areas, i.e., dorsolateral prefrontal cortex (BA 9/46), middle cingulate gyrus, and caudate nucleus. Recruitment of a distinct corticolimbic network for visual memory in the elderly suggests that age-related neurobiological deterioration not only results in focal changes but also in the modification of large-scale network operations.

Key words: aging; functional connectivity; hippocampus; partial least squares; short-term memory; structural equation modeling; visual memory; plasticity

There is consensus about the critical role of the hippocampus in declarative memory (Milner, 1978; Squire and Zola-Morgan, 1991; Eichenbaum et al., 1996; Tulving and Markowitsch, 1998). There is also little doubt that memory capacities dependent on hippocampal processing decline with age. Until recently, memory decay in the elderly was thought to originate in deficient hippocampal processing associated with its anatomical deterioration. However, neuroanatomical studies demonstrating no changes in hippocampal cell number and size across age have questioned this old hypothesis (Sullivan et al., 1995; Rapp and Gallagher, 1996; Morrison and Hof, 1997). Recently, Smith et al. (1999) have shown that age-related structural degeneration occurs in subcortical neuronal populations of the basal forebrain, which constitute a major cholinergic input to neocortex. Thus, loss of critical subcortical afferents, together with age-related molecular changes in receptor number and dendritic arborization (Morrison and Hof, 1997), may act to disrupt hippocampal physiology (Barnes, 1979; Barnes and McNaughton, 1980; Bach et al., 1999) and consequently, memory performance (Grady et al., 1995; Gallagher and Rapp, 1997; Tanila et al., 1997a,b). Given the current scenario, examination of functional interactions between the hippocampus and its afferents is critical for understanding the basis of age-related memory decline.

The integrity of functional interactions can be assessed through the study of interregional covariances of activity, which allows the examination of how activity in a brain area affects and is affected by activity changes in related areas (McIntosh, 1999). Application of covariance analysis to human neuroimaging data has shown that age modifies the functional interactions subserving episodic memory (Cabeza et al., 1997a,b; Grady et al., 1999). Age-related differences in neural interactions between hippocampus and cingulate gyrus, and hippocampus and dorsolateral prefrontal cortex have also been documented during episodic and working memory tasks, respectively (Grady et al., 1995; Esposito et al., 1999). However, many of these studies have compared groups on tasks in which there is an age-related performance difference. Interpretation of the results under these circumstances may be confounded because one cannot disambiguate differences related to deficits in performance from differences related to aging per se.

We have examined the effect of age on the functional connections of the hippocampus underlying equal performance on a short-term visual memory task. Young and old subjects performed a delayed visual discrimination task in which they had to determine which of two successively presented sine wave gratings had the higher spatial frequency (McIntosh et al., 1999b). The focus of this paper was to assess whether equal behavioral performance in young and old subjects was supported by the same corticolimbic functional interactions. To foreshadow, our results indicate that equivalent behavioral performance in young and old subjects is supported by different corticolimbic networks.

MATERIALS AND METHODS

Experimental procedure. The experimental design for this study has been described elsewhere (McIntosh et al., 1999b). Briefly, 10 young (average age, 23; average years of education, 13) and nine old (average age, 65; average years of education, 14.5) subjects were positron emission tomography (PET)-scanned while performing a visual delayed-discrimination task. Subjects were screened to ensure none suffered from medical, neurological, or psychiatric disorders before participation and were informed of all the risks of the experimental procedure before giving written consent; they were paid for participation. The experimental protocol was approved by the Human Subjects Use Committee of Baycrest Center at the University of Toronto.

The task required a discrimination between successively presented sine wave gratings based on spatial frequency. Two gratings of spatial frequency, f and $f + \Delta f$, were presented sequentially in each trial. The base frequency, f, varied randomly across trials across a ± 0.25 log unit range, centered 1.9 cycles/°. This low spatial frequency range minimized contrast sensitivity differences related to age. Grating contrast was modulated by a circular envelope 5.25° in diameter; contrast was 20% within the envelope

Received March 31, 2000; revised July 17, 2000; accepted Aug. 25, 2000.

This work was supported by the Alzheimer's Association of America, the Natural Sciences and Engineering Research Council of Canada, and the Medical Research Council of Canada.

Correspondence should be addressed to Dr. Valeria Della-Maggiore, Rotman Research Institute of Baycrest Centre, 3560 Bathurst Street, Toronto, Ontario M6A 2E1, Canada. E-mail: valeria@psych.utoronto.ca.

 0270-6474/00/208410-07$15.00/0

and 0 outside the envelope. The side (right or left) and the order in which the higher frequency grating appeared on the screen were randomized across trials. Subjects responded by pressing a right or a left key according to the location of the selected grating on the screen. The time interval between stimulus presentations (ISI) was varied to examine the decay in visual memory.

In the initial testing session, the magnitude of the spatial frequency difference was varied across trials, and the percentage of correct responses was recorded for each difference. Discrimination thresholds were estimated by fitting Weibull functions to each participant's data for each ISI. Thresholds were defined as the spatial frequency difference that produced correct responses in 80% of the trials. The next day, during scanning, each subject was tested with four different values of Δf, which ranged from 5% below that subjects discrimination threshold, to 5% above, in increments of 2.5%. To ensure the number of stimuli presented during a scan session constant across subjects, a deadline procedure was used: all subjects were instructed to respond within 1500 msec after the offset of the second grating. Trials with reaction times longer than 1500 msec would have been discarded, although this did not occur for any subject.

PET scans were obtained using a protocol described elsewhere (Cabeza et al., 1997a). Eight PET scans were obtained after a bolus injection of 40 mCi $[^{15}O]H_2O$ for each scan. Images were acquired over 60 sec using a GEMS-Scanditronix PC2048–15B head scanner (in-plane resolution 5–6 mm), and measurements began when the bolus tracer arrived to the head. The interscan interval was 11 min. Radioactive counts were used as an indirect indication of regional cerebral blood flow (rCBF).

All subject's images were spatially transformed to facilitate intersubject averaging and identification of common areas of change. For a subject, all image volumes were registered to the initial scan to correct for head motion across the experiment (AIR software). The images were then transformed to an rCBF template conforming to a standard brain atlas space (Talairach and Tournoux, 1988) and smoothed with a 10 mm isotropic Gaussian filter to reduce individual anatomic variability (SPM95; Friston, 1995). Voxel values within a transformed image volume were then expressed as a ratio of the average counts for all brain voxels within a scan. There were no group differences in whole brain average counts, which justifies the ratio adjustment.

Participants were PET-scanned during performance with 0, 500, and 4000 msec ISI. The simultaneous task (0 msec ISI; "simultaneous-discrimination control") was designed to control for comparative and decision-related processing necessary to perform the present task. The remaining scans were controls for trial density differences between different ISI conditions.

Network analysis. The experimental questions focused on the interactions among brain regions and their relation to performance in the visual discrimination task. Network analysis provides the most direct way of answering these questions (McIntosh, 1999), and therefore was the approach of choice. The steps used in the present paper can be conceptually summarized as follows: a distributed pattern of activity that directly related to behavior was identified using multivariate partial least squares (PLS) (McIntosh et al., 1996a). Behavioral PLS identifies distributed patterns that, as a whole, relate to some aspect of performance—e.g., group or task similarities and group or task differences. This analysis was the focus of a previous report and is summarized in Results (McIntosh et al., 1999b).

Next, from the distributed patterns identified by PLS, we targeted a hippocampal region to begin answering the questions for the present study. The first experimental question we asked was whether the functional connections (Friston et al., 1993) of the hippocampus with the rest of the brain were equivalent across young and old subjects. PLS (in this case a "seed-voxel" or seed PLS) was used to address this question because it is optimized to identify distributed patterns rather than single voxels. The seed PLS analysis of functional connectivity was then supplemented with covariance structural equation modeling (CSEM) or path analysis (McIntosh and Gonzalez-Lima, 1994; McIntosh et al., 1994; Nyberg et al., 1996). CSEM combines information about the anatomical pathways and the functional connectivity to provide a measure of effective connectivity (Friston et al., 1993) among a set of brain regions, or how brain areas directly affect one another. In a sense, CSEM expresses the interactions among regions within a more realistic neuroanatomical context.

Partial least squares. A full description of PLS can be found elsewhere (McIntosh et al., 1996a; McIntosh, 1999) and is summarized here. Behavioral PLS analysis was used in this study to identify patterns of brain areas whose relation with behavioral performance differed across groups. Based on the covariance between rCBF and behavioral performance, PLS extracts a discrete number of latent variables (LV) that best reflects the brain–behavior relationship. This procedure comprises three steps. First, correlation between behavior and rCBF values at each voxel are computed across subjects and within task. This produces one correlation map per condition for each group. Second, the correlation maps are put into a matrix and analyzed with singular value decomposition. This produces mutually orthogonal LVs, each one consisting of a singular image and a singular profile. Singular images contain a weighted linear combination of voxels that as a whole covary with behavior across groups. The numerical weights within the image are called saliences and can be positive or negative. The singular profile indicates the nature of the brain–behavior covariance (see below). Third, multiplication of the singular image by the raw images (dot-product) for each subject results in individual brain scores. The brain score is an indication of how much of the pattern represented in a singular image is expressed by a subject within a condition and is conceptually similar to a factor score from a factor analysis. The correlation between behavioral performance and brain scores across subjects within each scan produces scan profiles, which are proportional to the singular profiles from SVD but have a simpler interpretation because they are correlations. These scan profiles can be represented by scatter plots. If the scan profiles indicate a similar correlation across tasks or groups, salient areas in the singular image will show a similar correlation with behavior across tasks or groups. If scan profiles differ between tasks or groups, then the singular image will reflect a task or group difference in brain–behavior correlations.

The behavior PLS was used to select the hippocampal voxel of interest. To address the issue of functional connectivity, the hippocampal voxel was used in a seed-voxel PLS (McIntosh et al., 1997; McIntosh, Rajah and Lobaugh 1999), which is identical to a behavior PLS except that subject rCBF at the voxel of interest is used rather than behavior. Thus, the seed PLS identifies distributed patterns of activity that are functionally connected with the hippocampus. The scan profiles from this analysis indicate whether the functional connections are similar or different across groups and tasks.

For both behavioral and seed PLS, the reliability of voxel saliences in the singular image and the significance of the correlation profiles within and between groups were assessed by bootstrap estimation of the SE ($p < 0.01$) and permutation ($p < 0.05$), respectively (McIntosh and Gonzalez-Lima, 1998; McIntosh, Rajah and Lobaugh, 1999). In interpreting the singular images, voxels were considered reliable if they had a ratio of salience to SE greater than three (Efron and Tibshirani, 1986).

Covariance structural equation modeling. For the construction of the neural networks, voxels identified by the seed PLS were selected based on their bootstrap ratio and their functional relevance to visual memory (as described in the literature on visual memory and related tasks; Orban and Vogels, 1998; Orban et al., 1998). The anatomical projections among the nodes of the network were determined based on the neuroanatomy of nonhuman primates (Petrides and Pandya, 1988; Pandya and Yeterian, 1990; Knierim and Van Essen, 1992, Gloor et al., 1993; Arikuni et al., 1994; Bachevalier et al., 1997).

The interregional correlations and anatomical pathways among selected brain areas were used as the input to compute path coefficients with the computer program LISREL 8.3 (Joreskog and Sorbom, Scientific Software International Inc, 1999). Path coefficients are numerical weights assigned to the anatomical connections. Their magnitude and nature (i.e., inhibitory or excitatory; Nyberg et al., 1996) are represented in the figures by the thickness and type of connecting arrows (i.e., dashed or solid), respectively. Significant differences across groups were assessed using the stacked model approach (McIntosh et al., 1994). The process involves statistically comparing functional models in which path coefficients are constrained to be equal between groups (null model) with those in which the coefficients are allowed to differ (alternative model). The comparison of models is done by subtracting the goodness-of-fit χ^2 value for the alternative model from the χ^2 value for the null model. If the alternative model has a significantly lower χ^2 value then the functional models are statistically different between groups. This χ^2_{diff} is assessed with the degrees of freedom equal to the difference in the degrees of freedom for the alternative and null model.

Because the voxels used for CSEM were identified as belonging to a pattern of functional connections that distinguished groups, the statistical assessment in CSEM is redundant. However, CSEM provides an anatomical framework to interpret the differences between groups. Functional connectivity differences can arise from direct influences or through mediated influences. These possibilities were investigated with CSEM.

RESULTS

Psychophysical results showed a main effect of task on discrimination thresholds with no main effect of group or task by group interaction (McIntosh et al., 1999b), indicating that discrimination thresholds were equal for young and old subjects [500 msec (mean ± SE): young = 0.07 ± 0.005, range, 0.04–0.12; old = 0.06 ± 0.008, range, 0.04–0.10; 4000 msec: young = 0.14 ± 0.01, range, 0.08–0.20; old = 0.14 ± 0.02, range, 0.05–0.26]. During scanning, subjects produced correct responses on 79.2% of all trials, which confirms the accuracy as well as the stability of day one threshold measurements. Reaction time did not differ across groups.

Behavioral PLS

Three significant LVs were obtained from the behavioral PLS (McIntosh et al., 1999b). One LV identified a set of brain regions whose rCBF correlated similarly with behavior across tasks and groups ($r = 0.78$ for young-500 msec; $r = 0.41$ for young-4000 msec; $r = 0.68$ for old-500 msec; and $r = 0.79$ for old-4000 msec). The

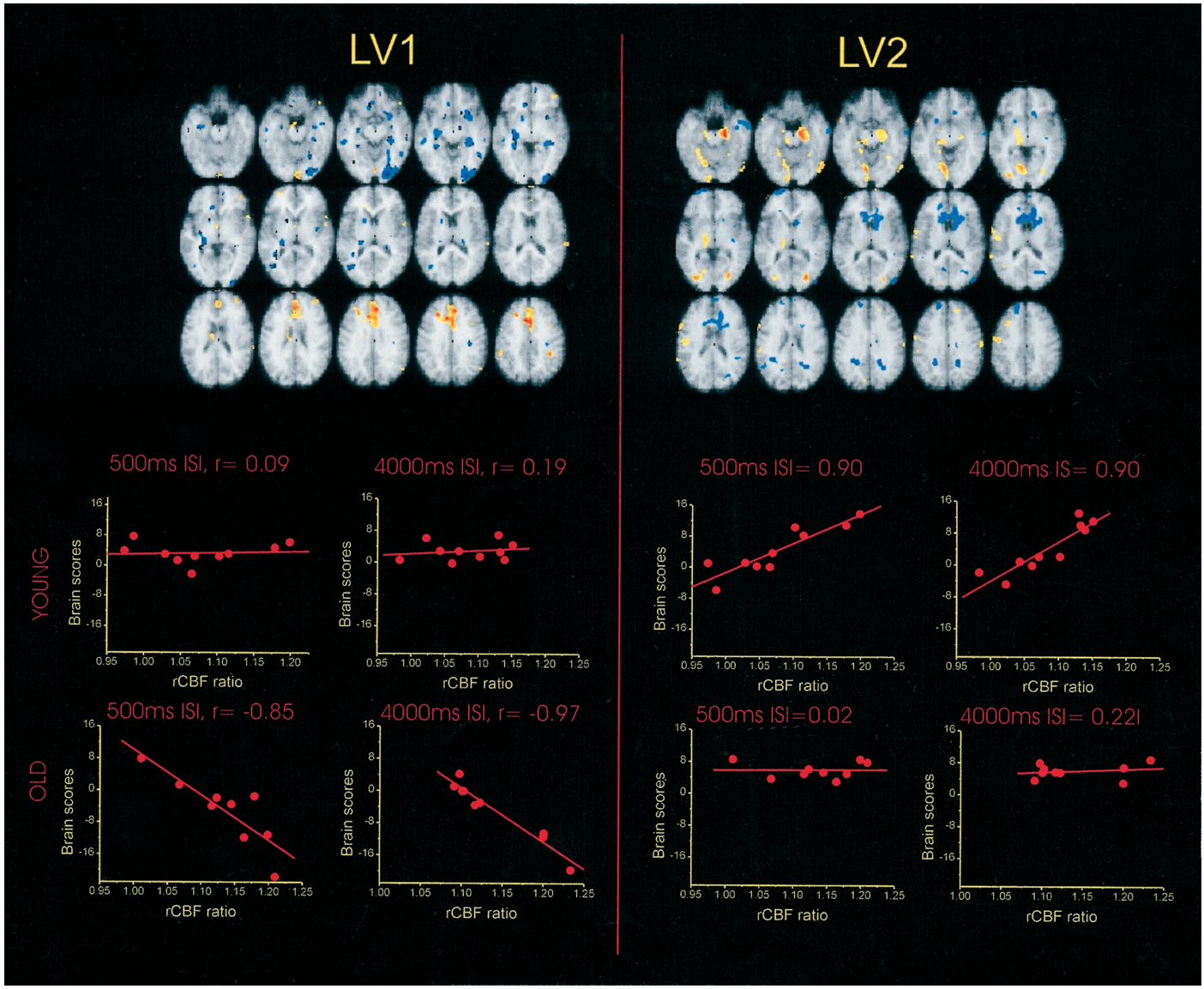

Figure 1. Seed PLS analysis. Shown are the singular images (*top*) corresponding to LV1 and LV2 and scan profiles (*bottom*) (correlation of brain scores and rCBF of RHIPP) for young and old subjects. Brain scores were obtained from the product of the singular image and each subject's image. Brain regions whose activity correlated positively with the pattern shown in the scan profile (positive saliences) are depicted in the singular image in *red*, whereas brain regions whose activity correlated negatively with the pattern shown in the scan profile (negative saliences) are depicted in the singular image in *blue*. Correlation coefficients between brain scores and RHIPP rCBF are displayed for each plot as *r*. MRI brain slices for the singular images are in standard atlas space (Talairach, 1988) and range from 20 mm ventral (*top left*) to 36 mm dorsal (*bottom right*) to the anterior commissure–posterior commissure line, with increments of 4 mm.

right hippocampus was highly salient in the singular image for this LV and was further investigated for its functional connections, as indicated below. The coordinates for this region according to the Talairach and Tournoux (1988) stereotaxic atlas of the human brain were: $x = 20; y = -18; z = -12$. The other two LVs identified a main effect of task, distinguishing the brain–behavior correlations between 500 and 4000 msec ISI for both groups and a group-by-task interaction in which the distinction between 500 and 4000 msec ISI was different for the groups. A complete discussion of these latter two LVs can be found in our previous report (McIntosh et al., 1999b).

The rCBF in the right hippocampal (RHIPP) region was somewhat higher for old subjects, although not statistically significant, and did not show task-dependent activity changes (1.07 ± 0.07 for young-500 msec; 1.083 ± 0.05 for young-4000 msec; 1.13 ± 0.06 for old-500 msec; and 1.14 ± 0.05 for old-4000 msec). The correlation of the RHIPP with behavior ($r = -0.67$ for young-500 msec; $r = -0.1$ for young-4000 msec; $r = -0.69$ for old-500 msec; and $r = -0.36$ for old-4000 msec; i.e., increases in hippocampus rCBF relate to decreased psychophysical threshold) was similar across tasks and groups.

Seed-voxel PLS

The seed-voxel PLS analysis for RHIPP identified two significant latent variables, LV1 and LV2. The scan profiles shown as scatter plots are depicted at the bottom of Figure 1 and indicate that the pattern of brain areas identified by LV1 was highly correlated with RHIPP in old subjects ($r = -0.85$ for old-500 msec and $r = -0.97$ for old-4000 msec), but much less so in young subjects ($r = 0.09$ for young-500 msec and $r = 0.19$ for young-4000 msec). Conversely, the pattern of brain areas identified by LV2 was highly correlated with RHIPP in young subjects ($r = 0.90$ for young-500 msec and $r = 0.90$ for young-4000 msec), but much less so in old subjects ($r = 0.02$ for old-500 msec and $r = 0.22$ for old-4000 msec). Peak positive saliences for LV1 were located in the left superior frontal gyrus [Brodmann's area (BA) 9/46] and bilateral middle cingulate gyrus, whereas peak negative saliences were located in the temporal gyrus, inferior temporal gyrus, and caudate nucleus (Table 1). Peak

Table 1. Brain areas identified by seed-voxel PLS analysis whose activity covaried with RHIPP activity

	Voxel #	Y-500	Y-4000	O-500	O-4000	Bootstrap ratio	*x*	*y*	*z*	Brain region	BA
LV1	1	—	—	—	—	—	20	−18	−12	Hippocampus	
	2	−0.13	0.35	−0.88	−0.88	4.61	−28	30	28	Superior frontal gyrus	9/46
	3	0.04	0.26	−0.78	−0.81	5.13	0	16	36	Cingulate gyrus	32
	4	0.09	0.18	−0.82	−0.76	4.56	−2	36	24	Gdf/cing	9
	5	−0.27	−0.11	0.93	0.63	−3.40	−50	8	−24	Middle temporal gyrus	21
	6	−0.32	−0.38	0.94	0.71	−5.08	−40	−70	8	Inferior temporal gyrus	19
	7	−0.29	−0.01	0.85	0.61	−3.82	−18	8	8	Caudate nucleus	
LV2	1	—	—	—	—	—	20	−18	−12	Hippocampus	
	2	0.48	0.75	−0.06	−0.09	3.91	−18	−42	−8	Parahippocampal gyrus	35/36
	3	0.82	0.79	0.20	0.08	5.37	−32	−82	0	Fusiform gyrus	18/19
	4	0.66	0.81	0.17	0.19	5.76	22	−78	4	Fusiform gyrus	18/19
	5	0.53	0.83	−0.30	−0.35	4.33	−32	20	36	Middle frontal gyrus	8
	6	−0.72	−0.39	0.07	−0.07	−2.81	54	−20	−24	Inferior temporal gyrus	20
	7	−0.83	−0.86	0.17	−0.56	−6.14	−18	64	0	Superior frontal gyrus	10
	8	−0.75	−0.56	0.57	0.49	−3.34	36	−6	−20	Middle temporal gyrus	20
	9	−0.70	−0.71	0.37	−0.06	−3.37	−46	−52	24	Inferior parietal gyrus	39
	10	−0.55	−0.84	0.00	−0.51	−5.02	−24	−48	28	Posterior cingulate	23/31
	11	−0.44	−0.87	0.05	0.191	−4.83	14	−46	32	Posterior cingulate	23/31

Shown are the stereotaxic coordinates corresponding to the peak voxels identified by LV1 and LV2, the corresponding Brodmann's area, and the voxel number that corresponds to the position of the voxel in the correlation matrices depicted in Figure 2. Columns labeled as Y-500, Y-4000, O-500, and O-4000 indicate the correlation of each voxel with RHIPP for the corresponding conditions. Bootstrap ratio is the parameter estimate for each voxel over its SE (for details refer to Materials and Methods).

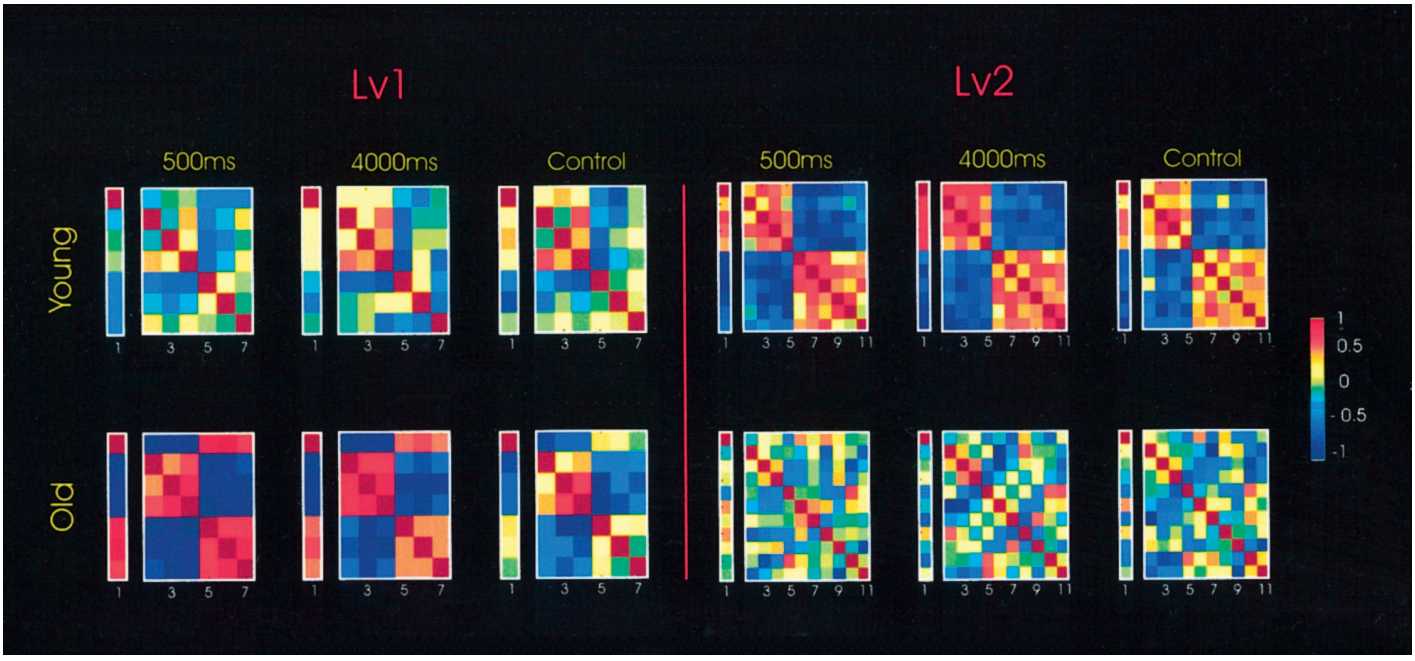

Figure 2. Functional connectivity of the corticolimbic regions depicted in Table 1. Six correlation matrices are displayed for each LV: (1) interregional correlations for young subjects, 500 msec delay condition, (2) interregional correlations for young subjects, 4000 msec delay condition, (3) their corresponding simultaneous-discrimination control, (4) interregional correlations for old subjects, 500 msec delay condition, (5) interregional correlations for old subjects, 4000 msec delay condition, and (6) their corresponding simultaneous-discrimination controls. The *column numbers* on each symmetrical matrix correspond to the brain areas listed in Table 1. Correlation coefficients are represented as color gradations (*red* = positive, and *blue* = negative). The correlation coefficients of RHIPP with the rest of the brain areas are shown on the *first column* on the left. The other columns depict the correlation coefficients for the remaining voxels of the table.

positive saliences for LV2 were found in hippocampus and bilateral fusiform gyrus, whereas peak negative saliences were found in left superior frontal gyrus (BA 10) and bilateral posterior cingulate gyrus (Table 1).

To better appreciate the functional connections of RHIPP, we examined the interregional correlations among peak voxels identified by LV1 and LV2 of the seed PLS results. Correlation coefficients obtained from this analysis were color-coded according to their magnitude and sign and are shown in Figure 2. The first column on the left represents the correlations of RHIPP with the other brain regions, and remaining columns are the correlations among the voxels. Confirming the results obtained from the seed PLS, the interregional correlations obtained for the peak voxels identified by LV1 were much stronger in old subjects than in young subjects, whereas those obtained for the peak voxels identified by LV2 were much stronger in young subjects than in old subjects.

To evaluate whether the pattern of interregional correlations were memory-specific, we compared the voxel correlations in the

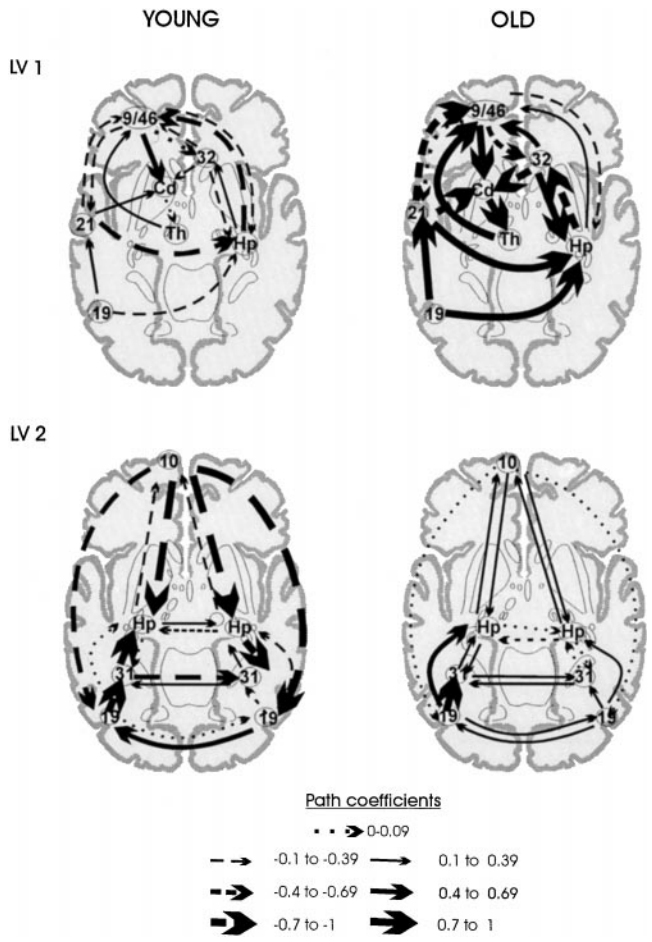

Figure 3. Functional models for young and old subjects obtained from regions identified by LV1 and LV2 based on the 500 msec delay condition. The sign and magnitude of the path coefficients are represented in the graphs by the type of arrow (*dashed arrows,* inhibitory influences; *solid arrows,* excitatory influences) and its thickness, respectively. Paths in which the coefficients were close to zero are depicted as *dotted arrows*. The anatomical location of some brain areas is distorted to maintain figure clarity.

delay conditions with the correlations among the same voxels measured during the simultaneous-discrimination control task. Statistical assessment by permutation tests (McIntosh et al., 1999b) indicated that the brain patterns showing high interregional correlations in old subjects were statistically different from the control condition (for LV1, $p = 0.002$ for old-500 msec vs simultaneous-discrimination control, $p = 0.002$ for old-4000 msec vs simultaneous-discrimination control), whereas the pattern showing high interregional correlations in young subjects were similar to the control condition (for LV2, $p = 0.97$ for young-500 msec vs simultaneous-discrimination control, $p = 0.96$ for young-4000 msec vs simultaneous-discrimination control).

Structural equation modeling covariance

Two different anatomical models were built because the results of the seed PLS suggested that different hippocampal networks were recruited by each group. Given that no delay-related differences were found for the functional connections among peak voxels depicted in Table 1, only the data from the 500 msec condition was used to construct the models. One model was based on the regions identified by LV1, which were regions strongly correlated in old subjects; the other model was based on the regions identified by LV2, which were strongly correlated in young subjects (Fig. 3). Of the voxels used in the correlational analysis, seven voxels were selected to construct the neural networks. This choice was made according to the criteria described in Materials and Methods. The seed voxel, RHIPP, was included in both models. The examination of rCBF responses in the present and other related PET studies showed that activity in the right hippocampus is highly correlated with activity in neighboring medial temporal lobe structures, such as subiculum, posterior entorhinal, and perirhinal cortex. These correlations partly reflect autocorrelation because of smoothing of the images (McIntosh et al., 1996a, 1997). As a result, our designation of RHIPP should be understood to include contributions from the hippocampus proper and the other aforementioned medial temporal regions. All anatomical projections included in the models correspond to monosynaptic pathways described in the monkey literature (for details, see Materials and Methods).

High correlations between areas identified by PLS led to path coefficient estimates that were much greater than one, which could compromise the model stability. To obviate stability concerns, any path coefficients with estimated values greater than one (absolute value) were fixed at ± 0.95. Statistical comparisons between groups were then made with these constraints imposed. From the model constructed for the old subjects (LV1), the path coefficients corresponding from left (L) inferior temporal gyrus to RHIPP and from L middle temporal gyrus to RHIPP were fixed to 0.95, whereas those from L superior frontal gyrus to L caudate and from RHIPP to R cingulate gyrus were fixed to -0.95.

The omnibus comparison for the anatomical model built using the peak voxels from LV1 revealed a significant difference in effective connectivity between groups ($\chi^2_{diff}(12) = 64.85$; $p < 0.005$). Figure 3*a* shows the path coefficients for the young group and those for the old group. In accordance with results from the correlational analysis, the strength of neural connections in the old subjects was much higher than in their young counterparts.

Likewise, the omnibus comparison for the anatomical model built using the peak voxels from LV2 showed a significant difference in effective connectivity between groups ($\chi^2_{diff}(20) = 41.08$; $p < 0.005$). Figure 3*b* depicts the path coefficients for the two groups. Notice that this network consisted of more posterior regions than the network depicted in Figure 3*a*. Contrary to the pattern obtained for LV1, and in accordance with the correlational analysis, the strength of neural connections in the young subjects was much higher than in their old counterparts.

DISCUSSION

The present study demonstrates that the cortical regions functionally associated with the RHIPP differed between young and old subjects. The stronger functional connections obtained in old participants for the corticolimbic network based on LV1 and in young participants for the network based on LV2 suggest the existence of a distinct hippocampal neural network subserving visual memory in the elderly.

Despite the growing research aimed at identifying molecular, anatomical, and physiological markers of aging (Rapp and Gallagher, 1996; Smith et al., 1999), the impact of late ontogenetic changes on information processing at different organizational levels of the brain (neuron, neuronal ensemble, neural network) remains largely unknown. We have shown that the type and magnitude of functional interactions among corticolimbic neuronal ensembles change dramatically with age. Furthermore, because equivalent behavior rules out differences in performance as a possible confound, we hypothesize that the neural network underlying performance in old subjects resulted from functional reorganization of corticolimbic circuits.

Although the hippocampal voxel selected for this seed PLS analysis showed no age-related differences in average rCBF, its interaction with other cortical areas varied significantly across groups. This finding suggests that to understand the relation of a given brain region (in this case, RHIPP) with performance, that region needs to be considered in the context of the other coactive, functionally connected regions, i.e., in its neural context (McIntosh, 1999). Thus, modification of the hippocampal neural context due to age-related changes such as reduced subcortical afferents, dendritic arborization, and receptor number (Morrison and Hof,

1997), may result in deficient information processing, and depending on the task demands, in memory decline.

Age-related changes in information coding by the hippocampus have been recently demonstrated by Tanila et al. (1997a) at the single cell level. Electrophysiological recording from rats performing a radial maze task indicated that hippocampal place cells of young rats created new spatial representations in novel environments (different environmental cues), whereas place fields of memory-impaired and memory-unimpaired old rats maintained the same spatial representations in new and familiar environments. Given that basic firing properties of hippocampal place fields (i.e., spatial selectivity, reliability, and directional specificity) were similar across age, the authors have hypothesized that differential encoding must have resulted from changes in brain regions afferent to the hippocampus. Likewise, Barnes et al. (1997) have shown that although hippocampal place field maps of young rats were equally accurate and stable within and between water maze sessions, place field maps of old rats were rearranged between sessions. The results suggest that old rats may be impaired in the selection of the correct "cognitive map" rather than in maintaining the map once it has been selected, a hypothesis that finds support in the age-related impairment in hippocampal LTP (Barnes, 1979).

Deficient hippocampal encoding also has been postulated to underlie age-related modifications of hippocampal interactions in humans performing cognitive-demanding memory tasks. Grady et al. (1995) have shown that during encoding of episodic memory, rCBF of the right hippocampus was most strongly correlated with anterior cingulate in the young and with the left parahippocampal gyrus in the old. In addition, Esposito et al. (1999) have reported age-related changes in the functional connections between the right hippocampus (RH) and left dorsolateral prefrontal cortex (LDPFC) during performance on working memory tasks. These two regions were correlated in old subjects but not in their young counterparts during performance on Raven's progressive matrices task, whereas they were correlated in young subjects but uncorrelated in old subjects during performance on the Wisconsin Card-Sorting test. These results suggest that age-related changes in the functional interactions of the hippocampus underlie performance on a variety of cognitive tasks.

An alternative to the hypothesis of functional reorganization is that old subjects used other encoding strategies as a compensatory mechanism to optimize performance (Grady et al., 1999). A change in sensory-processing strategy has been suggested by some studies showing that aged animals rely more on local than on distal cues to learn a maze (Barnes et al., 1987; Tanila et al., 1997b). Because this behavior was also reported after fimbria-fornix lesions, it has been suggested that such change in strategy may partly originate in age-related disruption of hippocampal function (Tanila et al., 1997a). Additional support for this hypothesis comes from Pascalis and Bachevalier (1999), who have shown that although monkeys with neonatal hippocampal lesions perform as well as controls on a DNSM task, they are severely impaired by introducing a distractor during the delay intervals. The absence of a similar deficit in the controls suggest that hippocampectomized animals use a different strategy to perform correctly in the DNMS task. Although we cannot conclusively dismiss a strategy difference between groups, the use of simple abstract stimuli without semantic content, together with the lack of a group difference in verbalizable task strategy and subjective difficulty in our study (as indexed by postexperiment debriefing, McIntosh et al., 1999b), renders this alternative explanation unlikely.

In the present study we examined the participation of the RHIPP and related brain areas in short-term visual memory. Assessment of task-related effects indicated that the functional connectivity of corticolimbic areas recruited by old subjects was stronger for the 500 msec ISI condition than for the 0 msec ISI condition. These differences were less pronounced in young subjects. These results suggest that whereas recruitment of the hippocampus and related cortical areas is necessary for visual memory in old subjects, in young subjects it is related to the visual discrimination component of the task.

A substantial number of studies have shown hippocampal involvement in nondeclarative memory paradigms, including short-term memory and nonmnemonic tasks. Selective lesion of the hippocampus has been shown to impair visual recognition in monkeys performing a visual paired-comparison tasks for delay intervals longer than 8–10 sec (Pascalis and Bachevalier, 1999; Zola et al., 2000). Delay, match, and nonmatch-selective single-unit activity has been reported in hippocampal cells during performance on short-term memory paradigms in rats and primates (Colombo and Gross, 1994; Haxby et al., 1995; Wiebe and Staubli, 1999). Likewise, electrophysiological assessment through depth electrodes in humans has revealed task-related changes in hippocampal activity associated with visual encoding during object categorization, familiarity, perceptual matching, and working memory (Seeck et al., 1995). Using event-related functional neuroimaging, Buchel et al. (1999) reported differential responses (CS+ vs CS−) of hippocampal activity during aversive trace conditioning in humans. Another neuroimaging study from Beason-Held et al. (1998) indicated a time-dependent increase in hippocampal activity during feature extraction compared with elementary form perception of abstract stimuli. Finally, a role of the hippocampus in motor regulation has also been proposed based on the temporal correlation between hippocampal slow wave activity and spontaneous voluntary motor activities in rats (for review, see Vanderwolf and Cain, 1994). Together with the results discussed above, the outcomes from our study support the participation of the hippocampus in mnemonic and nonmnemonic processes and further suggest that the degree of hippocampal involvement in memory processing may vary as a result of functional reorganization induced by age.

Conclusion

The finding of a distinct neural network associated with the right hippocampus during visual memory suggests that neurobiological deterioration associated with late ontogeny not only results in focal changes but also in the modification of the functional connectivity of the brain. In some cases, such as in our findings and some lesion studies (Buckner et al., 1996), reorganization of neural circuitry may lead to functional compensation and hence preserved performance. However, in other cases, anatomical reorganization may interfere with the normal functioning of other brain regions and therefore hinder unrelated behaviors (Grady et al., 1995). Finally, it is possible that increases in task demands weakens the aged brain's ability to compensate, leading to cognitive decline. Investigation of the biological processes underlying anatomical and functional reorganization is a major imperative to understand and eventually alleviate some of the cognitive deficits accompanying late ontogenetic changes.

REFERENCES

Arikuni T, Sako H, Murata A (1994) Ipsilateral connections of the anterior cingulate cortex with the frontal and medial temporal cortices in the macaque monkey. Neurosci Res 21:19–39.

Bach ME, Barad M, Son H, Zhuo M, Lu, YF, Shih R, Mansuy I, Hawkins RD, Kandel ER (1999) Age-related defects in spatial memory are correlated with defects in the late phase of hippocampal long-term potentiation in vitro and are attenuated by drugs that enhance the cAMP signaling pathway. Proc Natl Acad Sci USA 96:5280–5285.

Bachevalier J, Meunier M, Lu MX, Ungerleider LG (1997) Thalamic and temporal cortex input to medial prefrontal cortex in rhesus monkeys. Exp Brain Res 115:430–444.

Barnes CA (1979) Memory deficits associated with senescence: a neurophysiological and behavioral study in the rat. J Comp Physiol 931:74:104.

Barnes CA, McNaughton BL (1980) Physiological compensation for loss of afferent synapses in rat hippocampal granule cells during senescence. J Physiol (Lond) 309:473–485.

Barnes CA, Green EJ, Baldwin J, Johnson WE (1987) Behavioural and neurophysiological examples of functional sparing in senescent rat. Can J Psychol 41:131–140.

Barnes CA, Suster MS, Shen J, McNaughton BL (1997) Multistability of cognitive maps in the hippocampus of old rats. Nature 388:272–275.

Beason-Held LL, Purpura KP, Van Meter JW, Azari NP, Mangot DJ, Optican LM, Mentis MJ, Alexander GE, Grady CL, Horwitz B, Rapoport SI, Schapiro MB (1998) PET reveals occipitotemporal pathway

activation during elementary form perception in humans. Vis Neurosci 15:503–510.
Buchel C, Dolan RJ, Armony JL, Friston KJ (1999) Amygdala-hippocampal involvement in human aversive trace conditioning revealed through event-related functional magnetic resonance imaging. J Neurosci 19:10869–10876.
Buckner RL, Corbetta M, Schatz J, Raichle ME, Petersen SE (1996) Preserved speech abilities and compensation following prefrontal damage. Proc Natl Acad Sci USA 93:1249–1253.
Cabeza R, Grady CL, Nyberg L, McIntosh AR, Tulving E, Kapur S, Jennings JM, Houle S, Craik FI (1997a) Age-related differences in neural activity during memory encoding and retrieval: a positron emission tomography study. J Neurosci 17:391–400.
Cabeza R, McIntosh AR, Tulving E, Nyberg L, Grady CL (1997b) Age-related differences in effective neural connectivity during encoding and recall. NeuroReport 8:3479–3483.
Cave CB, Squire LR (1992) Intact verbal and nonverbal short-term memory following damage to the human hippocampus. Hippocampus 2:151–163.
Colombo M, Gross CG (1994) Responses of inferior temporal cortex and hippocampal neurons during delayed matching to sample in monkeys (*Macaca fascicularis*). Behav Neurosci 108:443–455.
Efron B, Tibshirani R (1986) Bootstrap methods for standard errors, confidence intervals and other measures of statistical accuracy. Stat Sci 1:54–77.
Eichenbaum H, Schoenbaum G, Young B, Bunsey M (1996) Functional organization of the hippocampal memory system. Proc Natl Acad Sci USA 93:13500–13507.
Esposito G, Kirkby BS, Van Horn JD, Ellmore TM, Berman KF (1999) Context-dependent, neural system-specific neurophysiological concomitants of aging: mapping PET correlates during cognitive activation. Brain 122:963–979.
Friston KJ (1995) Statistical parametric mapping: oncology and current issues. J Cereb Blood Flow Metab 15:361–370.
Friston KJ, Frith CD, Liddle PF, Frackowiak RSJ (1993) Functional connectivity: the principal-component analysis of large (PET) data sets. J Cereb Blood Flow Metab 13:5–14.
Gallagher M, Rapp PR (1997) The use of animal models to study the effects of aging on cognition. Annu Rev Psychol 48:339–370.
Gloor P, Salanova V, Olivier A, Quesney LF (1993) The human dorsal hippocampal commissure. Brain 116:1249–1273.
Grady CL, McIntosh AR, Horwitz B, Maisog JM, Ungerleider LG, Mentis MJ, Pietrini P, Schapiro MB, Haxby JV (1995) Age-related reductions in human recognition memory due to impaired encoding. Science 269:218–221.
Grady CL, McIntosh AR, Rajah MN, Beig S, Craik FI (1999) The effects of age on the neural correlates of episodic encoding. Cereb Cortex 9:805–814.
Haxby J, Ungerleider LG, Horwitz B, Rapoport SI, Grady CL (1995) Hemispheric differences in neural systems for face working memory: a PET-rCBF study. Hum Brain Mapp 3:68–82.
Knierim JJ, Van Essen DC (1992) Visual cortex: cartography, connectivity, and concurrent processing. Curr Opin Neurobiol 2:150–155.
McIntosh AR (1999) Mapping cognition to the brain through neural interactions. Memory 7:523–548.
McIntosh AR, Gonzalez-Lima F (1994) Structural equation modeling and its application to network analysis in functional brain imaging. Hum Brain Mapp 2:2–22.
McIntosh AR, Gonzalez-Lima F (1998) Large-scale functional connectivity in associative learning: interrelations of the rat auditory, visual and limbic systems. J Neurophysiol 80:3148–3162.
McIntosh AR, Grady CL, Ungerleider LG, Haxby JV, Rapoport SI, Horwitz B (1994) Network analysis of cortical visual pathways mapped with PET. J Neurosci 14:655–666.
McIntosh AR, Bookstein FL, Haxby JV, Grady CL (1996a) Spatial pattern analysis of functional brain images using partial least squares. NeuroImage 3:143–157.
McIntosh AR, Grady CL, Haxby JV, Ungerleider LG, Horwitz B (1996b) Changes in limbic and prefrontal functional interactions in a working memory task for faces. Cereb Cortex 6:571–584.
McIntosh AR, Nyberg L, Bookstein FL, Tulving E (1997) Differential functional connectivity of prefrontal and medial temporal cortices during episodic memory retrieval. Hum Brain Mapp 5:323–327.
McIntosh AR, Rajah MN, Lobaugh NJ (1999a) Interactions of prefrontal cortex related to awareness in sensory learning. Science 284:1531–1533.
McIntosh A, Sekuler AB, Penpeci C, Rajah MN, Grady CL, Sekuler R, Bennett PJ (1999b) Recruitment of unique neural systems to support visual memory in normal aging. Curr Biol 9:1275–1278.
Milner B (1978) Clues to the cerebral organization of memory. In: Cerebral correlates of conscious experience (Buser PA, Rougeul-Buser A, eds), pp 139–153. Amsterdam: North-Holland.
Morrison JH, Hof PR (1997) Life and death of neurons in the aging brain. Science 278:412–419.
Nyberg L, McIntosh AR, Cabeza R, Nilsson LG, Houle S, Habib R, Tulving E (1996) Network analysis of positron emission tomography regional cerebral blood flow data: ensemble inhibition during episodic memory retrieval. J Neurosci 16:3753–3759.
Orban GA, Vogels R (1998) The neuronal machinery involved in successive orientation discrimination Prog Neurobiol 55:117–147.
Orban GA, Dupont P, De Bruyn B, Vandenberghe R, Rosier A, Mortelmans L (1998) Human brain activity related to speed discrimination tasks. Exp Brain Res 122:9–22.
Pandya DN, Yeterian EH (1990) Prefrontal cortex in relation to other areas in rhesus monkey: architecture and connections. Prog Brain Res 85:63–94.
Pascalis O, Bachevalier J (1999) Neonatal aspiration lesions of the hippocampal formation impair visual recognition memory when assessed by paired-comparison task but not by delayed nonmatching-to-sample task. Hippocampus 9:609–616.
Petrides M, Pandya DN (1988) Association fibers to the frontal cortex from the superior temporal region in the rhesus monkey. J Comp Neurol 273:52–66.
Rapp PR, Gallagher M (1996) Preserved neuron number in the hippocampus of aged rats with spatial learning deficits. Proc Natl Acad Sci USA 93:9926–9930.
Seeck M, Schomer D, Mainwaring N, Ives J, Dubuisson D, Blume H, Cosgrove R, Ransil BJ, Mesulam MM (1995) Selectively distributed processing of visual object recognition in the temporal and frontal lobes of the human brain. Ann Neurol 37:538–545.
Smith DE, Roberts J, Gage FH, Tuszynski MH (1999) Age-associated neuronal atrophy occurs in the primate brain and is reversible by growth factor gene therapy. Proc Natl Acad Sci USA 96:10893–10898.
Squire LR, Zola-Morgan S (1991) The medial temporal lobe memory system. Science 253:1380–1386.
Sullivan EV, Marsh L, Mathalon DH, Lim KO, Pfefferbaum A (1995) Age-related decline in MRI volumes of temporal lobe gray matter but not hippocampus. Neurobiol Aging 16:591–606.
Talairach J, Tournoux P (1988) Co-planar stereotaxic atlas of the human brain. Stuttgart: Thieme.
Tanila H, Shapiro M, Gallagher M, Eichenbaum H (1997a) Brain aging: changes in the nature of information coding by the hippocampus. J Neurosci 17:5155–5166.
Tanila H, Sipila P, Shapiro M, Eichenbaum H (1997b) Brain aging: impaired coding of novel environmental cues. J Neurosci 17:5167–5174.
Tulving E, Markowitsch HJ (1998) Episodic and declarative memory: role of the hippocampus. Hippocampus 8:198–204.
Vanderwolf CH, Cain DP (1994) The behavioral neurobiology of learning and memory: a conceptual reorientation. Brain Res Rev 19:264–297.
Wiebe SP, Staubli UV (1999) Dynamic filtering of recognition memory codes in the hippocampus. J Neurosci 19:10562–10574.
Zola SM, Squire LR, Teng E, Stefanacci L, Buffalo EA, Clark RE (2000) Impaired recognition memory in monkeys after damage limited to the hippocampal region. J Neurosci 20:461–463.